

# Assessment of the MODIS and AMSR-E-Derived SST Products in joining area of Asia and Indian-Pacific Ocean

**Yuxin Zhu<sup>a,b,c</sup>, Yanchen Bo<sup>a,c</sup>, Jiehai Cheng<sup>a,c,d</sup> and Jinzong Zhang<sup>b</sup>**

<sup>a</sup>School of Geography, Beijing Normal University, State Key Laboratory of Remote Sensing Science, jointly sponsored by Beijing Normal University and Institute of Remote Sensing Applications, Chinese Academy of Sciences, Beijing, China

<sup>b</sup>School of Urban and Environmental Sciences, Huaiyin Normal University, Jiangsu Province, China

<sup>c</sup>Beijing Key Laboratory for Remote Sensing of Environment and Digital Cities, Beijing Normal University, Beijing, China

<sup>d</sup>School of Surveying and Land Information Engineering, Henan Polytechnic University, Jiaozuo, Henan, China

(Manuscript received May 2012; revised July 2013)

The Moderate Resolution Imaging Spectroradiometer (MODIS) and the Advanced Microwave Scanning Radiometer (AMSR-E) aboard the NASA Earth Observation System's Aqua satellite have been measuring the sea surface temperature (SST) since 2002. Although satellite-derived SST data complement the ground-based SST field data in better understanding the role of SST in coupling the ocean and atmosphere, they need to be validated in order to determine the spatiotemporal variation of their availability, and their error features, and then to decide how they can be used for further applications. In this paper we assess the spatiotemporal coverage and error variation of MODIS and AMSR-E level-3 mapped SSTs during 2003 to 2005 over the joining area of Asia and the Indian-Pacific Ocean. Drifting buoy SST data obtained from the Atlantic Oceanographic and Meteorological Laboratory (AOML) is used as a benchmark for the study. The results show that multi-year and annual average availabilities of MODIS SSTs are lower than those of AMSR-E SSTs due to their different cloud penetration. Weekly mean availability of AMSR-E SSTs is nearly constant during 2003–2005 whereas that of MODIS SSTs shows obvious seasonal variation, i.e. it is low in summer and high in spring and autumn. The intra-annual variation of MODIS and AMSR-E availability is similar for the three year period. The geographical signal of annual mean availability of MODIS is more obvious than that of AMSR-E, i.e. it is high at about latitudes 20°N and 20°S and low around the equatorial regions. For error feature, the overall accuracy and precision of MODIS SSTs are lower than those of AMSR-E SSTs due to their slight differences in atmospheric effects, cloud penetration, spatial resolution, measured depths, and retrieval algorithms. Even so, annual mean biases of these two datasets are both within 0.5 °C. The intra-annual variation of the error feature of MODIS is much more obvious than that of AMSR-E due to the wider range of mean bias and standard deviation. The intra-annual variations of MODIS and AMSR-E error are similar for the three year period. We also find that the accuracy and precision of MODIS and AMSR-E have an obvious geographical signal for the three year period. That is, the accuracy and precision become higher moving from mid-latitudes of the northern hemisphere through equatorial regions to mid-latitudes of the southern hemisphere.

## Introduction

The sea surface temperature (SST) acts as an important parameter in coupling the ocean and atmosphere through exchanges of heat, momentum, moisture, and gases (Donlon et al. 2002). So the oceanic temperature variability is an indicator for climate change (Zhang et al. 2009). Satellite SST data with high accuracy and fine resolution are essential for accurate climate assessment and monitoring. SST has been routinely measured from ships, buoys and offshore platforms. However, these conventional measurements are usually sparse and cannot satisfy the needs of ocean research. The global satellite remotely-sensed SST, as an important complementary data source, has made a major contribution to climate research due to its superior spatial coverage and real-time availability. Satellite-derived SST products have been available from a number of sensors for about 30 years (Guan and Kawamura 2003). At present there are two main kinds of sensors: infrared and microwave sensors. Advanced Very High Resolution Radiometer (AVHRR), Moderate Resolution Imaging Spectroradiometer (MODIS), and Tropical Rainfall Measuring Mission (TRMM) Visible and Infrared Scanner (VIRS) are popular infrared sensors. The main microwave sensors include TRMM Microwave Imager (TMI), Advanced Microwave Scanning Radiometer (AMSR), and Advanced Microwave Scanning Radiometer for EOS (AMSR-E). Infrared products have higher spatial resolution but have many missing values because of contamination from cloud and aerosols. Microwave remote sensing SST products have higher spatial continuity than infrared products do but still suffer from contamination from high wind speed, high columnar water vapour, high cloud water content and rain (Wentz et al. 2000, Gentemann et al. 2004). The spatial resolutions of microwave remote sensing SST products are lower than those of infrared products. Though the satellite-derived SSTs are attractive due to their superior spatial coverage compared to conventional in-situ (ship and buoy) SSTs, they may have large biases (Reynolds 1993). In particular, although the globally averaged satellite-derived SSTs might have small biases, their regional and seasonal biases are larger than those of in-situ SSTs (Zhang et al. 2009). Therefore, satellite-derived SSTs need to be validated so as to evaluate their fitness of use for further applications. In this paper we focus on the assessment of infrared SST data (MODIS SST at 4 km) and microwave SST data (AMSR-E at 25 km) to demonstrate their spatiotemporal variations of error features and availabilities over the joining area of Asia and the Indian-Pacific Oceans, which covers from 30°S to 46°N and from 30°E to 180°E. We select this area as our study region because it is a key area for the short-term climate variation and prediction in China (Guoxiong et al. 2006).

Validations of satellite-derived SST products have been conducted for many satellite SST products such as AVHRR SST (Li et al. 2001, Guan and Kawamura 2003, Lee et al. 2005). TMI SST (Senan et al. 2001, Gentemann et al. 2003, Stammer et al. 2003, Gentemann et al. 2004), and AVHRR and TMI

SST (Sun et al. 2007, Qiu et al. 2009). There is only limited literature on the validation of MODIS (Sun et al. 2007) and AMSR-E (Kim et al. 2010) over the joining area of Asia and Indian-Pacific Ocean. In addition, most of the research on validation of satellite-derived SSTs focuses on availability, mean bias, and root mean square error at a certain time point. The spatiotemporal variations of the errors in satellite SST products have seldom been investigated. In this study we perform a spatiotemporal variation analysis and comparison analysis of the satellite SST products. Specifically, we assess the spatiotemporal variation of the availability of MODIS and AMSR-E SST data by the ratio of valid oceanic pixels and all oceanic pixels. We also investigate the spatiotemporal variation of the error features of MODIS and AMSR-E SST data using drifting buoy SST data obtained from the Atlantic Oceanographic and Meteorological Laboratory (AOML) as a benchmark in terms of mean bias, standard deviation and root mean square error during 2003 to 2005.

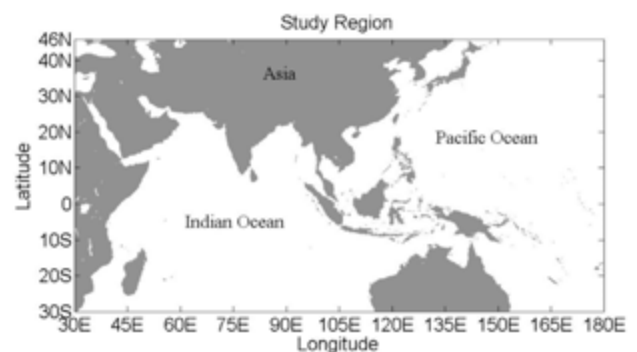
## Data

The geographical area of interest in this study is the rectangular area between latitudes 30°S and 46°N and between longitudes 30°E and 180°E, which covers the joining area of Asia and the Indian-Pacific Oceans (see Fig. 1). We select this area as our study region because it is a key area for short-term climate variation and prediction in China. The intra-seasonal and inter-annual oscillation of coupled ocean atmosphere system in this region has a direct impact on abnormal drought/flood in China (Guoxiong et al. 2006).

### Satellite-derived SST data

One of the satellite-derived SST datasets used in this study is from MODIS on the Aqua satellite. Currently the datasets are in HDF file format with 4 km and 9 km spatial resolutions and daily, 'weekly' (eight days), monthly and annual time intervals. We select the global level-3 mapped products with 4 km spatial resolution and eight-day temporal resolution during 2003 to 2005 for assessment. These SST data are produced at 0130 local time, so that the effect of diurnal warming of the surface ocean is minimised. These data are the latest science quality level-3 files processed and

Fig. 1. Study region.



distributed by the Ocean Biology Processing Group (OBPG) located at the NASA Goddard Space Flight Center (see [gcmd.nasa.gov](http://gcmd.nasa.gov)), and available at the website [oceandata.sci.gsfc.nasa.gov/MODISA/Mapped/](http://oceandata.sci.gsfc.nasa.gov/MODISA/Mapped/). The number of pixels in this study region is  $1824 \times 3600 = 6566400$ . Within one year, we have a total number of 46 images. The period of the first 45 'weeks' is eight days, but the last week is five days in non-leap years and six days in leap years. MODIS and drifting buoy measured SSTs have slightly different depths in the upper ocean, since the empirical coefficients in the MODIS SST retrieval algorithm are derived by regression analysis between MODIS thermal infrared brightness temperatures and the collocated in-situ SST observations from drifting and moored buoys. Measurements from the M-AERI in-situ radiometer are then used to convert the regressed SST to a skin SST measurement (approximately  $-0.2$  °C adjustment) at a depth of 0.01 mm, classified based on Donlon, Minnett et al. (2002) and Donlon and GHRSS-PP Science Team (2005) (see [ftp://podaac.jpl.nasa.gov/.../MODIS\\_SST\\_Guide\\_Doc.pdf](http://podaac.jpl.nasa.gov/.../MODIS_SST_Guide_Doc.pdf)). A detailed description of the MODIS SST retrieval algorithm is available at the website [modis.gsfc.nasa.gov](http://modis.gsfc.nasa.gov).

The passive microwave remote sensing SST data are derived from the AMSR-E sensor that was mounted onto NASA's Aqua satellite. The AMSR-E SST data were provided as daily maps, three-day mean maps, weekly mean maps, and monthly mean maps (see [www.remss.com](http://www.remss.com)). The AMSR-E SST data had been available since the 152nd day, 2002. They were produced and released by Remote Sensing Systems Inc supported by NASA (see [www.ssmi.com](http://www.ssmi.com)). In this paper, we select the version three AMSR-E SST products with daily time resolution and  $25 \times 25$  km spatial resolution, during the same time period with MODIS SST products for study. The AMSR-E SST data is available at [ftp://ftp.discover-earth.org/sst/daily/amsre/](http://ftp.discover-earth.org/sst/daily/amsre/). Using a simple empirical model of diurnal warming that depends on solar insolation, wind speed, and local time of observation (Gentemann et al. 2003), the AMSR-E daily SSTs were 'normalised' to a daily minimum SST, defined to occur at approximately 0800 local time (see [www.ssmi.com/sst/microwave\\_oi\\_sst\\_browse.html](http://www.ssmi.com/sst/microwave_oi_sst_browse.html)). AMSR-E measured the sub-skin temperature at approximately 1 mm depth (Dong et al. 2006). In this paper the AMSR-E SSTs are aggregated into eight-day temporal resolution by an averaging method to match up with MODIS SST data. Note that the last week is averaged over five days in non-leap years and six days in leap years. This is the same as for MODIS SSTs.

#### Drifting buoy measured SST data

Drifting buoy measured SSTs used in this study cover the period of 2003 to 2005 and are obtained from the Atlantic Oceanographic and Meteorological Laboratory (AOML) official website ([www.aoml.noaa.gov](http://www.aoml.noaa.gov)). They are used to validate the satellite-derived SSTs. We select drifting buoy SST observations at 0000 UTC to largely remove the effects of the ocean diurnal warm layer (Donlon et al. 2002). These buoy SST data are typically measured below the ocean

thermal skin (Minnett et al. 2011) at depths ranging from 0.2 m to 0.3 m. In the absence of diurnal warming, drifting buoy SSTs are representative of the SST derived from AMSR-E, and representative of the SST derived from MODIS with an approximate  $+0.2$  °C adjustment to account for the cool skin effect. We apply a gross error quality check into the drifting buoy SSTs for their quality control. The gross error check removed drifting buoy SST observations that are lower than  $-1.8$  °C or higher than  $35$  °C (Høyer et al. 2012). The drifting buoy SSTs are transformed into gridded data with the same spatiotemporal resolution as MODIS and AMSR-E SST data by a spatiotemporal averaging method. Specifically, we compute the mean of multi buoy SSTs in a  $0.04^\circ$  or  $0.25^\circ$  grid within eight days, respectively. This averaging procedure also reduces random error of buoy SSTs. We define the difference as satellite-derived SST minus (gridded) drifting buoy SST for further quality control on the drifting buoy observations. If the absolute value of difference is larger than  $10$  °C for both of the MODIS and AMSR-E, we regard the drifting buoy SSTs as the outlier and then they are removed.

## Evaluation of satellite-derived SST

Analyses using different in-situ observations and satellite-derived observations need a reference field. Some analyses use in-situ observations (ship and buoy) data as the benchmark, and other analyses may use a satellite-derived observation or a climatology (Reynolds et al. 2010). In this article we use drifting buoy observations as the benchmark.

#### Preprocessing of data

There are two issues we must resolve before the evaluation. One is the difference in temporal resolution between MODIS and AMSR-E: The temporal resolution of MODIS SST data is eight-day, and that of AMSR-E SST data is daily. The other is the representativeness of drifting buoy measurements. Because the heat capacity of sea water is very large the SST might not change significantly during a ten-day period (Abe 1984). Thus, in order to compare MODIS SSTs to AMSR-E SSTs, we first compute the eight-day means SST of AMSR-E using the time composite method. Secondly, the satellite-derived SST is an area/time mean measurement, whereas buoy SST is a point instantaneous measurement of the same physical system. As was mentioned earlier, the MODIS and AMSR-E SSTs, although measured at skin and sub-skin depths respectively, during night-time should agree closely with drifting buoy SSTs once the cool skin effect has been accounted for (Abe 1984, Donlon et al. 2002, Gentemann et al. 2003, Minnett et al. 2011). Considering these differences, drifting buoy SSTs at 0000 UTC are selected. In order to evaluate the satellite-derived eight-day mean SST, a standard eight-day mean in-situ SST should be provided. So we group the drifting buoy measurements by an eight-day interval. Note that the period of the last 'week' is not eight days; it is five days in non-leap years and six days in leap years. All available drifting buoy measurements located in a  $0.04^\circ$

and 0.25° grid during eight days are averaged to match the MODIS and AMSR-E SST spatial resolutions, respectively. Using such a multi-buoy average method the random error of the drifting buoy is partially removed.

### Evaluation of MODIS SST and AMSR-E SST

#### *Spatiotemporal features of availability*

The availability of the satellite SST, which is examined to ascertain the acceptance rate of all data, is defined as the ratio between the number of ocean pixels with observed SSTs and the number of all ocean pixels. The results are shown in Table 1. The multi-year averaged availability of MODIS SSTs is 70.427 per cent, which is lower than that of AMSR-E at 86.92 per cent. As is shown in Table 1, the annual mean availabilities of MODIS in this study region from 2003 through 2005 are 69.65 per cent, 71.48 per cent, and 70.15 per cent, respectively; the maximum and minimum weekly availabilities within a single year are 77.8215 per cent (39th week, early November) and 55.057 per cent (46th week, late December) in 2003, 81.6947 per cent (14th week, mid-April) and 60.9812 per cent (46th week, late December) in 2004, and 78.1074 per cent (15th week mid-April) and 55.2528 per cent (46th week, late December) in 2005. Note that for MODIS SSTs the minimum availability appears at 46th week (late December) in every year during this period 2003–2005. We find that the annual mean availabilities of AMSR-E SSTs are 86.78 per cent, 86.97 per cent, and 87.01 per cent, for the years of 2003, 2004, and 2005, respectively. Clearly, AMSR-E SSTs have much better annual mean availabilities than the MODIS SSTs do, which is expected because AMSR-E utilises the microwaves and possesses the advantage of cloud penetration. For AMSR-E SSTs, the maximum and minimum weekly availabilities within a single year are 86.9585 per cent (46th week, late December) and 86.5988 per cent (6th week, mid-February) in 2003, 87.0108 per cent (46th week, late December) and 86.8869 per cent (10th week, mid-March) in 2004, 87.0403 per cent (46th week, late December) and 86.9389 per cent (11th week, late March) in 2005. It is interesting to notice that in contrast to the MODIS SSTs, the maximum weekly availabilities of AMSR-E appear at the 46th week in all the three years 2003–2005.

**Table 1. The average annual and weekly maximal and minimal (within a year) availabilities during 2003–2005.**

Sensor		MODIS	AMSR-E	
Year	2003 (%)	Average	69.65	86.78
		Maximum	77.8215	86.9585
		Minimum	55.057	86.5988
	2004 (%)	Average	71.48	86.97
		Maximum	81.6947	87.0108
		Minimum	60.9812	86.8869
	2005 (%)	Average	70.15	87.01
		Maximum	78.1074	87.0403
		Minimum	55.2528	86.9389

Figure 2 shows the intra-annual temporal variation of weekly availabilities of two SST products: the weekly mean availability of AMSR-E is approximately constant from 2003 to 2005 (see Fig. 2 right panel), whereas the intra-annual temporal variation of the MODIS weekly availabilities is much larger (see Fig. 2 left panel). On the whole there are two wave crests in MODIS curves. The weekly averaged availability is low in the northern hemisphere summer and high in spring and autumn, and we find that this intra-annual temporal variation tendency is consistent in all the three years.

We also compute the weekly and annual mean availabilities of both SST products over grids in the same latitude at every 1° latitude band to investigate spatial variation of the availabilities. The results are shown in Fig. 3 and Fig. 4, where we can find obvious zonal characteristics for both MODIS SSTs and AMSR-E SSTs, and the changes of MODIS SSTs along the latitudes are more obvious than those of AMSR-E SSTs. As shown in Fig. 3, the latitude variation patterns of the annual mean availabilities of MODIS and AMSR-E SSTs do not change from year to year during this three-year period. From Fig. 3 we also find that the annual mean availability of AMSR-E SSTs is lower at low latitudes of the southern hemisphere than that at middle latitudes of the southern hemisphere due to the distribution of land. There is another zone where the annual mean availability of AMSR-E SSTs is low; at high latitudes of the northern hemisphere. The annual mean availability of MODIS SSTs (Fig. 3 left panel) shows a symmetrical distribution characteristic based on the equatorial axis. At mid-latitudes in either the northern or southern hemisphere, the annual mean availability is higher than those of other regions. This is because the availability of MODIS SSTs mainly depends on the existence of cloud. Higher availability is found in the mid-latitude (10°S–30°S and 10°N–30°N) zones with two temporal peaks of availability in every year (81.0747 per cent and 80.9197 per cent in 2003, 81.889 per cent and 81.7944 per cent in 2004, 83.77975 per cent and 82.9832 per cent in 2005). Low availability is found around the equatorial region and near 40°N with the lowest annual mean availability of 50.2127 per cent in 2003, 56.004 per cent in 2004, and 53.4082 per cent in 2005, respectively.

The spatial variation of weekly mean availability of MODIS SSTs at every 1° latitude band is more evident than that of AMSR-E SSTs (see Fig. 4). In the region between 10°N–10°S in latitude and region north to latitude 30°N, the weekly mean availabilities of MODIS SSTs are generally low. In the region between 10°N–30°N in latitude and the region that is south of latitude 10°S, the weekly mean availabilities of MODIS SSTs are generally high. The high availability zone between latitudes 10°N and 30°N has the tendency of moving to higher latitudes in the period between the 20th week (early May) and the 30th week (mid-August). The weekly mean availability of the AMSR-E SSTs is almost constant in each 1° latitude band. In regions south of latitudes 10°S and near latitude 30°N, the weekly mean availabilities are relatively high. However the weekly mean availabilities of regions

Fig. 2. The intra-annual temporal variations of the weekly mean availability from two products during 2003–2005 (left panel: MODIS; right panel: AMSR-E).

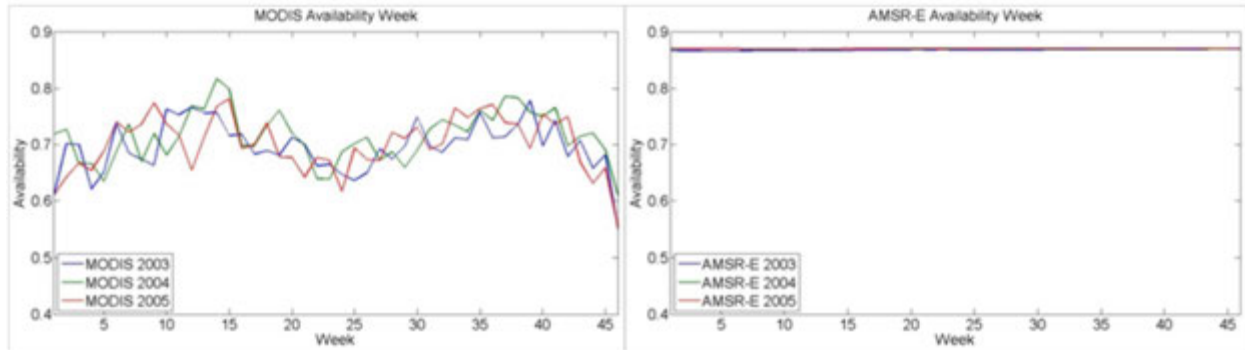
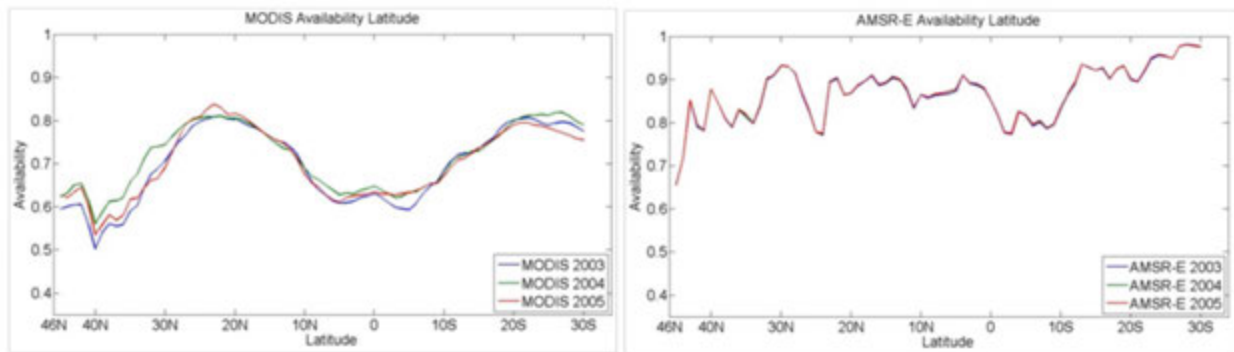


Fig. 3. Spatial variation of annual mean availability at different latitudes for MODIS and AMSR-E (left panel: MODIS; right panel: AMSR-E).



north of latitude 40°N are relatively low, since microwave SSTs retrieval is impacted by land.

#### Temporal variation of error feature

In this paper, the ‘accuracy’ and ‘precision’ of satellite-derived SST data are evaluated by using mean bias (satellite SST minus drifting buoy SST), standard deviation, and root mean square error (RMSE) compared with the drifting buoy SSTs. Buoy SST measurements are known to have high precision and can be used as a reference value (Aihua 2013). The numbers of SST measurements from buoys at 4 km are 41840, 55802, and 78110 in the years of 2003, 2004, and 2005, and those at 25 km are 32769, 42461, and 59520, respectively. Figure 5 shows the distribution of drifting buoys in the study region. It is worth noting that in 2003 there are no drifting buoy observations in Indonesian waters. In addition, there are few observations in the Pacific Ocean east of Japan in 2003 and in the northwest Indian Ocean in 2004. Zhang et al. (2009) studied the relationship between buoy density (defined as number of buoys/10° box) and potential satellite SST bias error and concluded that a buoy density of two was regarded as the minimum acceptable density. In this article the buoy density is defined as number of buoys/0.04° box and 0.25° box, respectively. So the buoy density in this study region is sufficient to validate the accuracy of satellite-derived SST (Aihua Li 2013).

Figure 6 is the scatter plots of satellite SSTs versus drifting

buoy SSTs. It can be seen that the satellite SSTs are largely consistent with the drifting buoy SSTs because dots scatter along the 1:1 line. However, the systematic error and random error of MODIS SSTs are larger than those of AMSR-E SSTs. In particular, the absolute mean bias and RMSE of MODIS SSTs are both larger than those of AMSR-E SSTs. Overall, MODIS SSTs are both cooler than that of drifting buoy SSTs because their annual mean biases are all negative, while AMSR-E SSTs are cooler than those of drifting buoy SSTs in 2004, and warmer than those of drifting buoy SSTs in 2003 and 2005. The MODIS SSTs are much cooler than drifting buoy SSTs relative to AMSR-E SSTs because the absolute mean bias of MODIS SSTs is larger than that of AMSR-E SSTs. This is because the MODIS SSTs are adjusted approximately  $-0.2^{\circ}\text{C}$  to represent skin SST. This can also be seen from scatter plots that the dots scattered along the 1:1 line for AMSR-E SSTs are more symmetrical than those for MODIS SSTs. It is worth noting that in low temperature regions, e.g. in regions colder than  $10^{\circ}\text{C}$ . MODIS SSTs are cooler than drifting buoy SSTs whereas AMSR-E SSTs are warmer than drifting buoy SSTs. The inter-annual variation of the error feature of these two SST products is not obvious.

The intra-annual variations of error features of the two satellite SSTs are shown in Fig. 7–9.

We find that the accuracy and the precision MODIS SSTs are lower than those of AMSR-E SSTs in each week (see

Fig. 4. The spatial variation of weekly mean availability in every 1° latitude band for MODIS and AMSR-E SSTs during 2003–2005 (left panel: MODIS, right panel: AMSR-E).

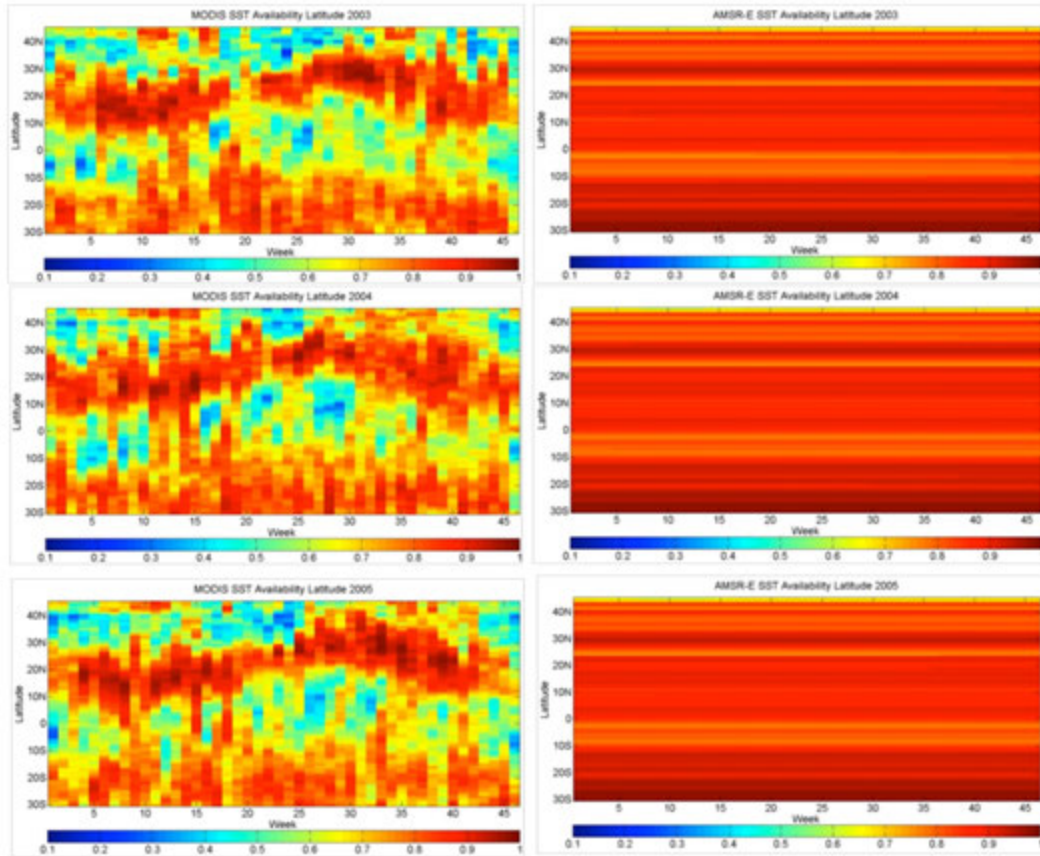


Fig. 5. The distribution of drifting buoys during 2003–2005 (a) 2003, (b) 2004, (c) 2005)

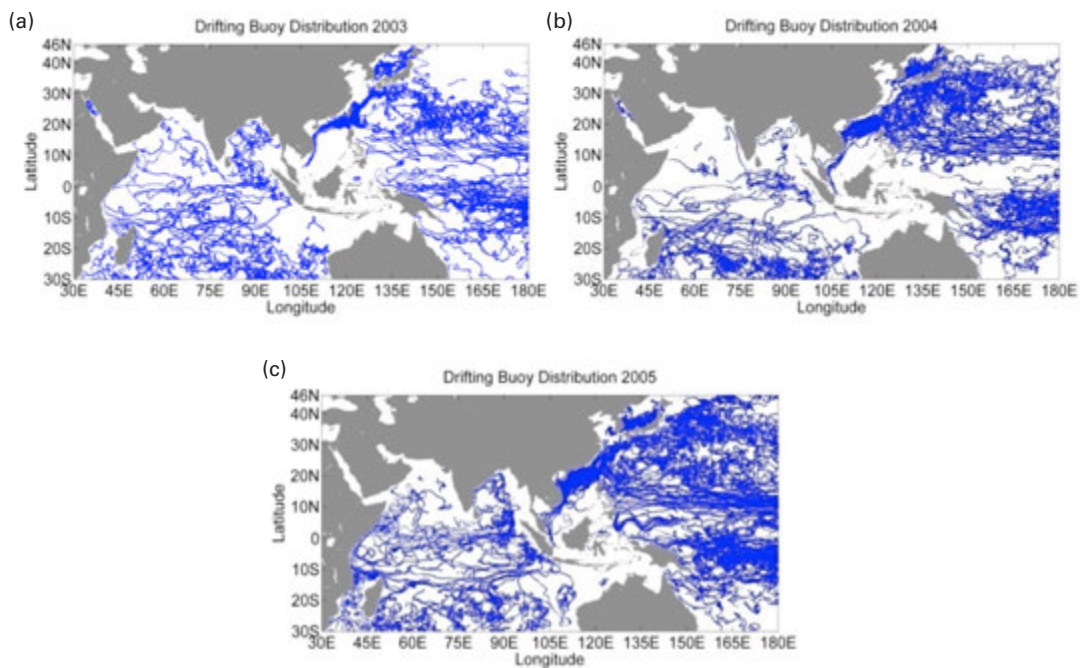


Fig. 6. Scatter plots of satellite SSTs against drifting buoy SSTs (a) MODIS 2003, (b) MODIS 2004, (c) MODIS 2005, (d) AMSR-E 2003, (e) AMSR-E 2004, (f) AMSR-E 2005.

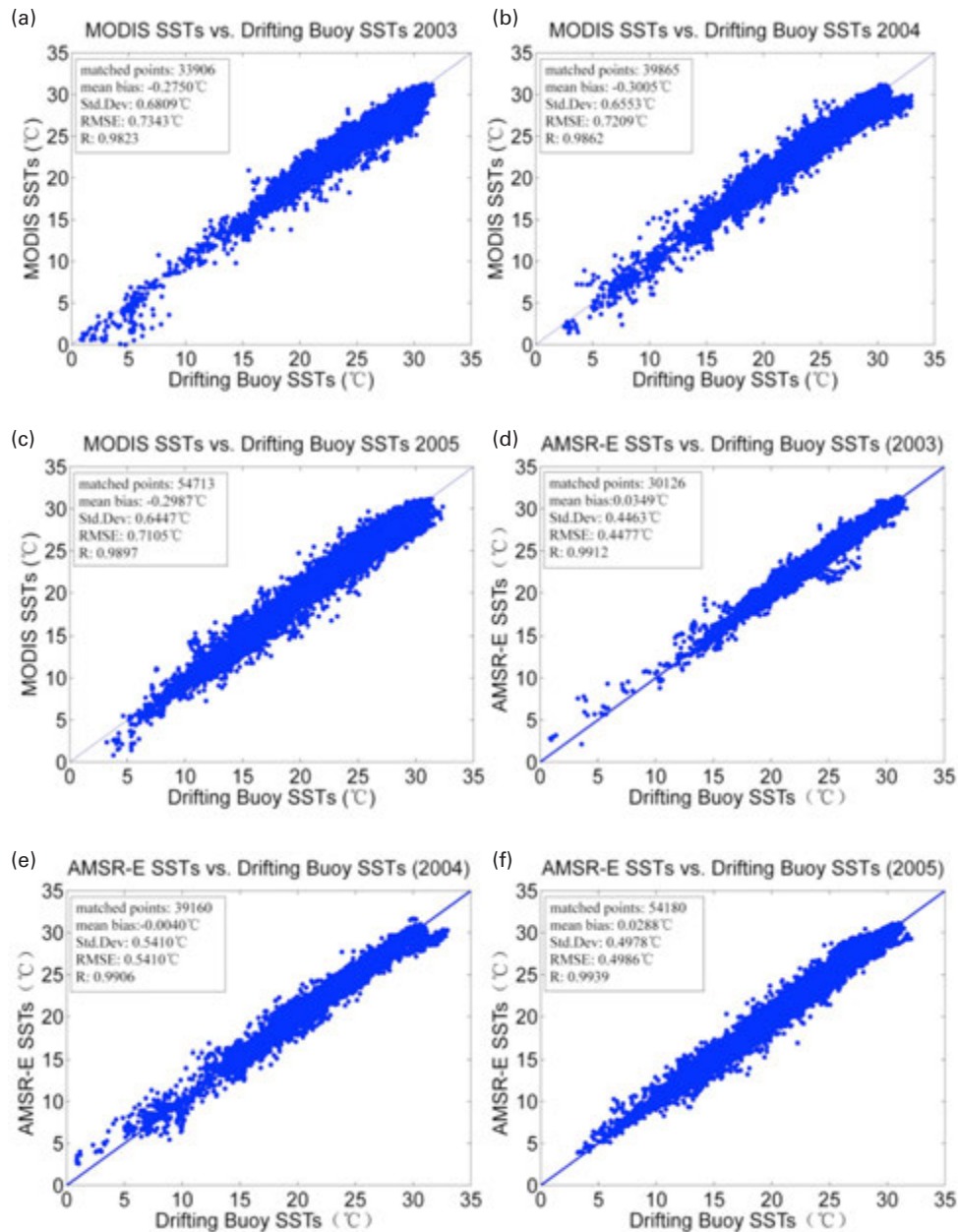


Fig. 7–9) because the absolute mean bias and the standard deviation of MODIS SSTs in each week are larger than those of AMSR-E SSTs, and the random error of MODIS SSTs in each week is also larger than that of AMSR-E SSTs (see Fig. 8). Intra-annual variation of the error feature of MODIS SSTs is much more obvious than that of AMSR-E SSTs. The mean bias ranges of MODIS and AMSR-E SSTs are 0.3448 °C and 0.2358 °C in 2003, 0.366 °C and 0.3337 °C in 2004, and 0.4141 °C and 0.2557 °C in 2005, respectively. The standard deviation ranges of MODIS and AMSR-E SSTs are 0.3025 °C and 0.214 °C in 2003, 0.2785 °C and 0.1696 °C in 2004, and 0.3137 °C and 0.3195 °C in 2005, respectively. The RMSE ranges of MODIS and AMSR-E SSTs are 0.3138 °C and

0.2154 °C in 2003, 0.3147 °C and 0.1734 °C in 2004, and 0.405 °C and 0.3194 °C in 2005, respectively. Though intra-annual variations of error features exist for both MODIS SSTs and AMSR-E SSTs, the intra-annual variation tendencies of the accuracy of MODIS SSTs and AMSR-E SSTs are similar for the three-year period. For MODIS SSTs, the accuracy during about 14th–20th weeks (mid-April–early June) is lower than those in the other weeks during 2003 to 2005; for AMSR-E SSTs, the accuracy during about 15th–30th weeks (late April–mid-August) is higher than those in other weeks during 2003 to 2005 (see Fig. 10). There is no obvious seasonality in standard deviation or root-mean-square error during the 2003–2005 period (Figs 11–12).

Fig. 7. Intra-annual variation of mean bias from two satellite SSTs: (a) 2003, (b) 2004 and (c) 2005.

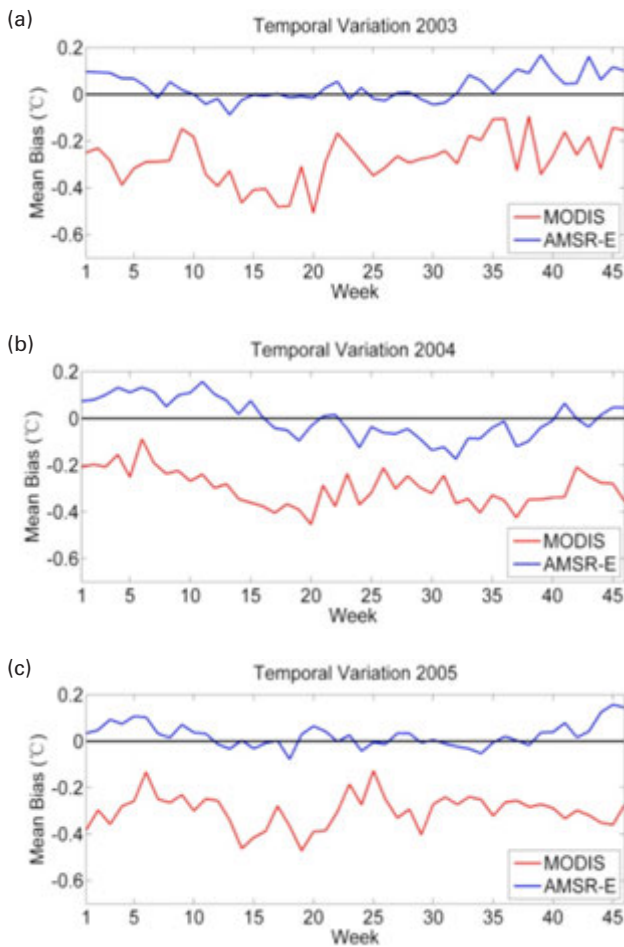
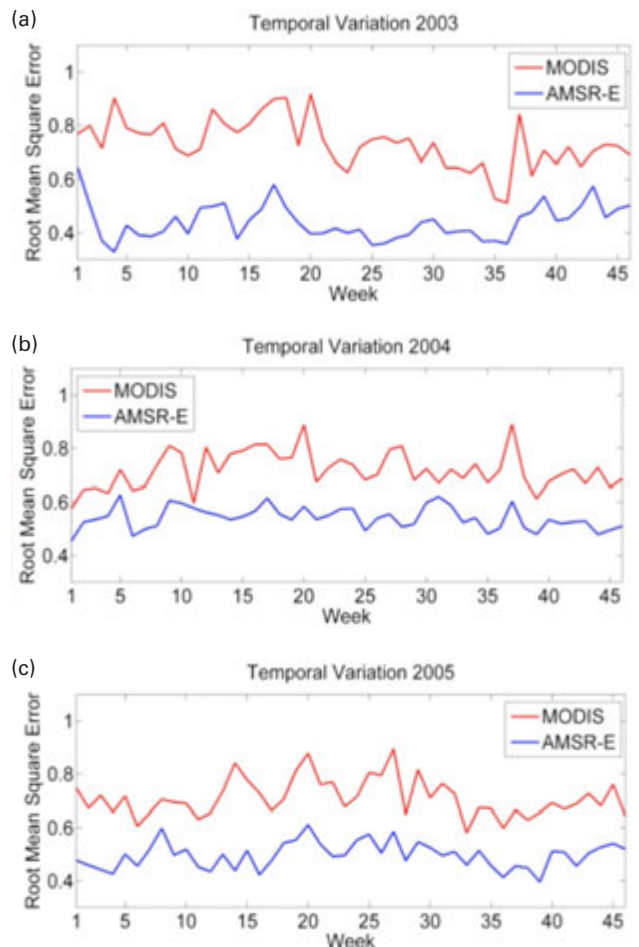


Fig. 8. Intra-annual variation of RMSE from two satellite SSTs: (a) 2003, (b) 2004 and (c) 2005.



*Spatial variation of error features*

In this section we focus on the spatial variation of error features of MODIS and AMSR-E SSTs. We compute the averages of mean bias, RMSE, and standard deviation in regions for every 1° latitude band. The results are shown in Figs 13–15.

As shown in Figs 13–15, the error features of MODIS SSTs and AMSR-E SSTs have an obvious geographical tendency. The accuracy and the precision both become higher moving from north to south, from higher latitudes of the northern hemisphere through equatorial regions to mid-latitudes of the southern hemisphere. The error standard deviation of MODIS SSTs is larger than that of AMSR-E SSTs for every 1° latitude region, and the RMSE of MODIS SSTs is higher than that of AMSR-E SSTs for every 1° latitude region, as can be seen from Figs 15 and 14, respectively. As shown in Fig. 13, during 2003 to 2005 MODIS SSTs are all cooler than those of drifting buoy SSTs for every 1° latitude region, whereas AMSR-E SSTs are cooler than those of drifting buoys with a few exceptions; bias of MODIS SSTs is mostly larger than that of AMSR-E SSTs for every 1° latitude region. We check the extent of variation of mean bias, RMSE, and standard

deviation at all latitudes. The mean bias range of MODIS SSTs and AMSR-E SSTs is 0.5726 °C and 0.4487 °C in 2003, 0.5663 °C and 0.6707 °C in 2004, and 0.5352 °C and 0.5092 °C in 2005, respectively; the standard deviation range is 0.4634 °C and 0.4480 °C in 2003, 0.4675 °C and 0.5317 °C in 2004, and 0.3817 °C and 0.4214 °C in 2005, respectively; and the RMSE range is 0.6641 °C and 0.5382 °C in 2003, 0.5557 °C and 0.7004 °C in 2004, 0.6668 °C and 0.4836 °C in 2005, respectively. This means that the extent of variation of accuracy, precision and random error of MODIS SSTs and AMSR-E SSTs at all latitudes are similar, and the degree of spatial variation of error features at all latitudes is larger than that of mean values during the three years. Even so, the inter-annual variation tendency of MODIS and AMSR-E error features are similar for the three-year period. This can be seen from Figs 16–18.

Fig. 9. Intra-annual variation of standard deviation from two satellite SSTs: (a) 2003, (b) 2004 and (c) 2005.

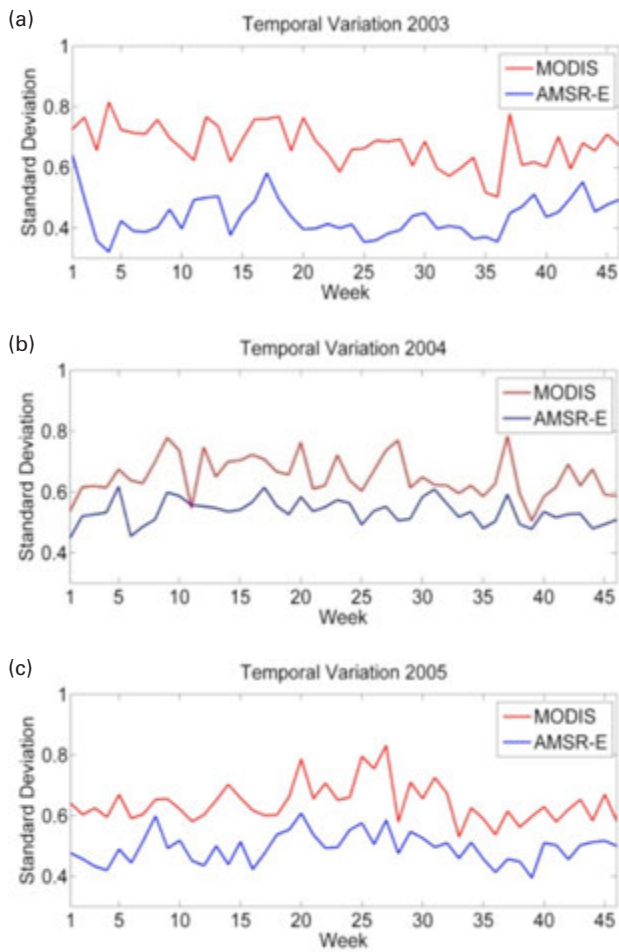


Fig. 10. Temporal tendency of mean bias in each year for MODIS SSTs and AMSR-E SSTs: (a) MODIS, (b) AMSR-E.

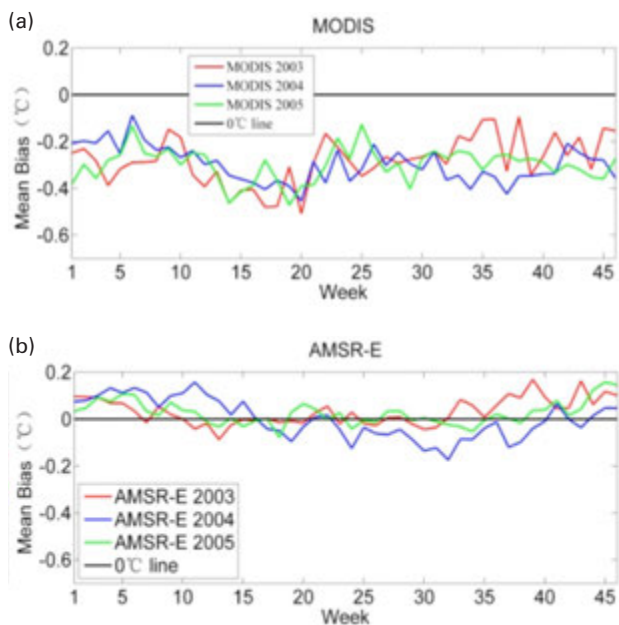


Fig. 11. Temporal tendency of RMSE in each year for MODIS SSTs and AMSR-E SSTs: (a) MODIS, (b) AMSR-E.

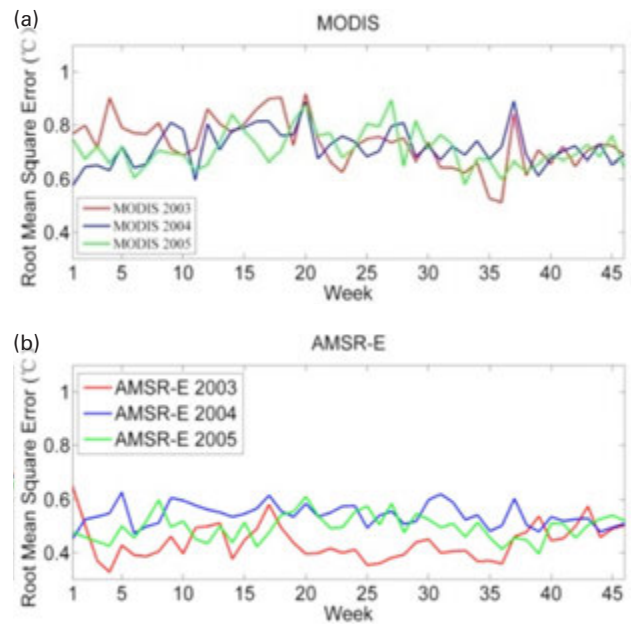


Fig. 12. Temporal tendency of standard deviation in each year for MODIS SSTs and AMSR-E SSTs: (a) MODIS, (b) AMSR-E.

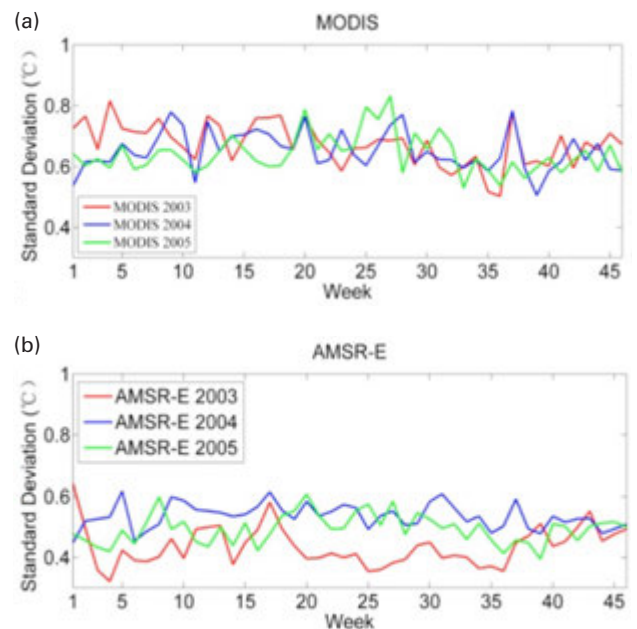


Fig. 13. Spatial variation of mean bias from two satellite SSTs: (a) 2003, (b) 2004, and (c) 2005.

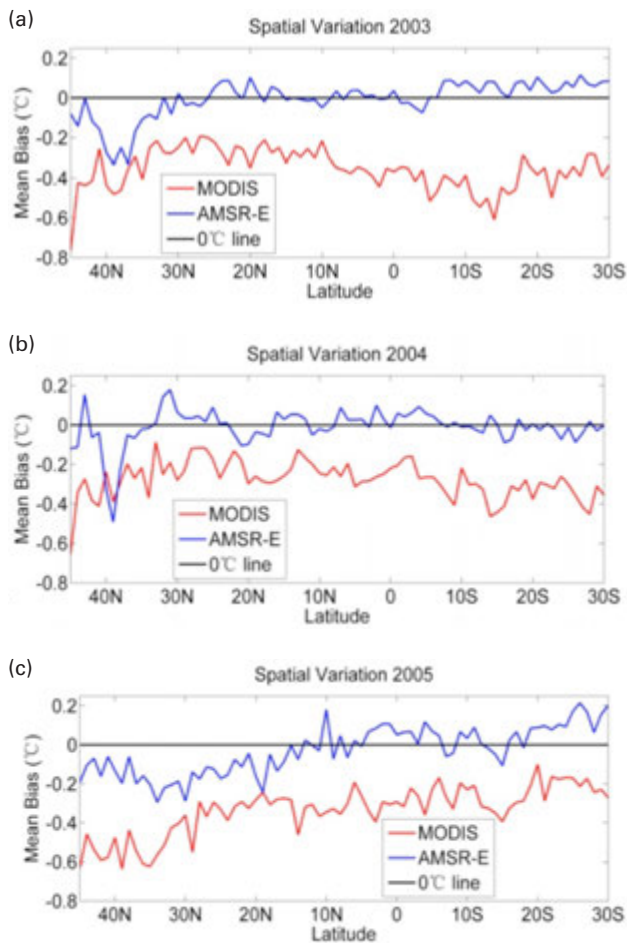
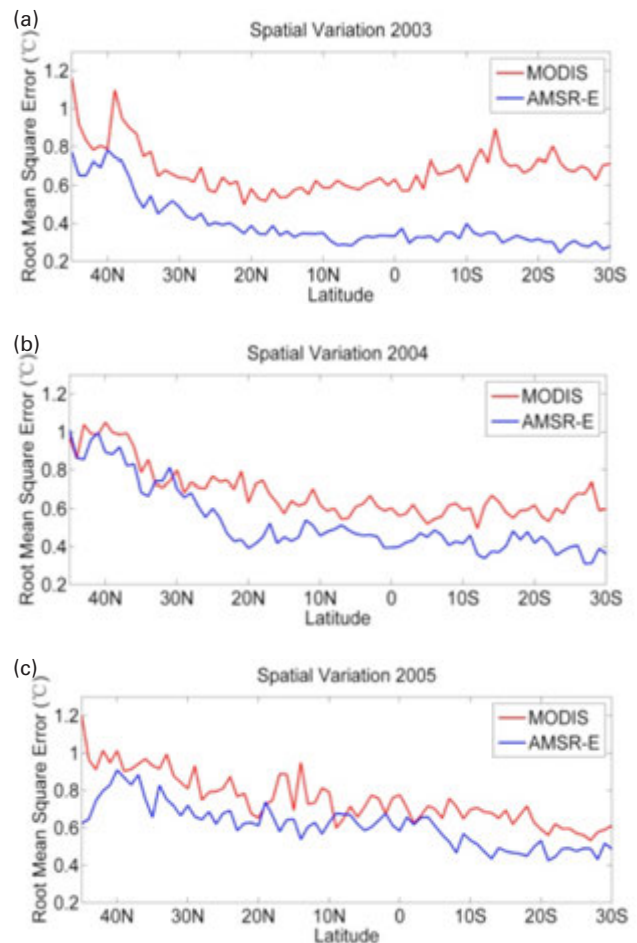


Fig. 14. Spatial variation of RMSE from two satellite SSTs: (a) 2003, (b) 2004, and (c) 2005.



## Summary

Accurate SST datasets are important in climate change and monitoring studies because SST is a key parameter in the atmospheric and oceanic coupling of heat, gas, and momentum (Dong et al. 2006). Satellite-derived SST has become an important data source due to its superior spatial-temporal coverage and real time measurements. However, infrared SST products suffer from cloud, water vapour, and aerosols contamination. All-weather measurements from microwave instruments complement the deficiency of infrared SST products. Due to the differences in atmospheric effects, cloud penetration, spatial resolution, the retrieval algorithm and the measured depth between MODIS and AMSR-E SST products, their uncertainties are different. As an important variable in ocean environment modeling and weather forecasting, error estimates of SST are necessary in ocean and weather data assimilation process and numerical weather simulation process. In this paper, we assess quantitatively the spatial coverages and the spatial-temporal error features of MODIS and AMSR-E SSTs in the area of the joining area of Asia and the Indian-Pacific Ocean during 2003 to 2005 using drifting buoy SST as benchmarks. The

main conclusions are as follows:

1. The spatial-temporal variation of availability is investigated. The weekly mean availability of AMSR-E SSTs is nearly constant for the three-year period due to its advantage of cloud penetration. Annual and multi-year averaged availabilities of MODIS SSTs are lower than those of AMSR-E SSTs, which is as expected since MODIS SSTs suffer from cloud contamination. The weekly mean availability of MODIS SSTs has larger temporal variation in a year than that of the AMSR-E SSTs does, which is consistent with the seasonal variation of cloud in the study region. We also find that the spatial variation of MODIS SSTs annual mean availability in each 1° latitude region is larger than that of AMSR-E SSTs. For MODIS SSTs in the equatorial region, the annual mean availability is obviously lower than that in other regions because there is more cloud cover in equatorial region than in other regions.
2. In our validation analysis of the satellite-derived SSTs using the drifting buoy SSTs as benchmark, we find that the accuracy and precision of MODIS SSTs are overall lower than those of AMSR-E SSTs during 2003 to 2005 due to their difference in atmospheric effects, cloud

Fig. 15. Spatial variation of standard deviation from two satellite SSTs: (a) 2003, (b) 2004, and (c) 2005.

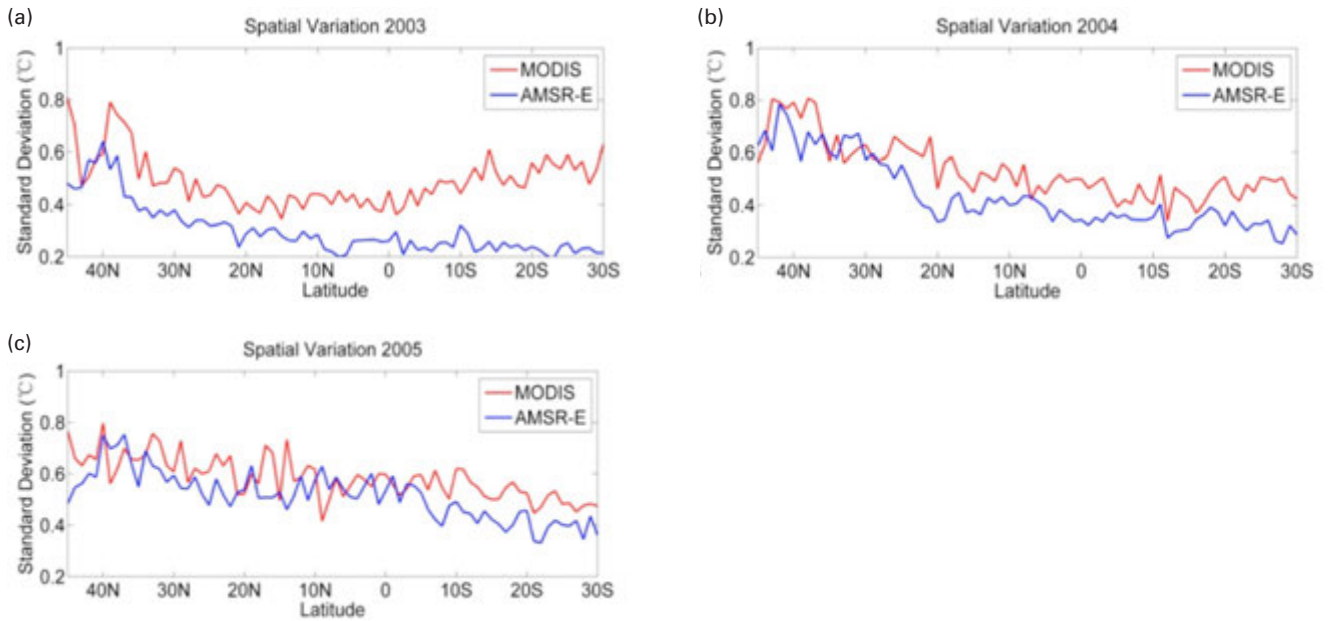


Fig. 16. Spatial tendency of mean bias in each year for MODIS SSTs and AMSR-E SSTs: (a) MODIS and (b) AMSR-E.

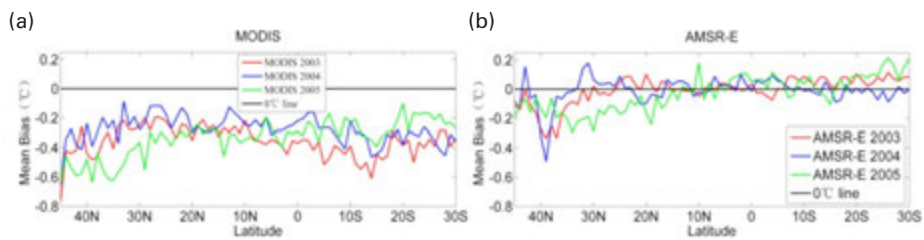


Fig. 17. Spatial tendency of standard deviation in each year for MODIS SSTs and AMSR-E SSTs: (a) MODIS and (b) AMSR-E.

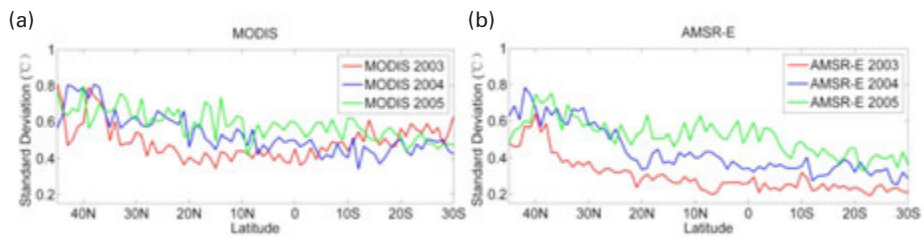
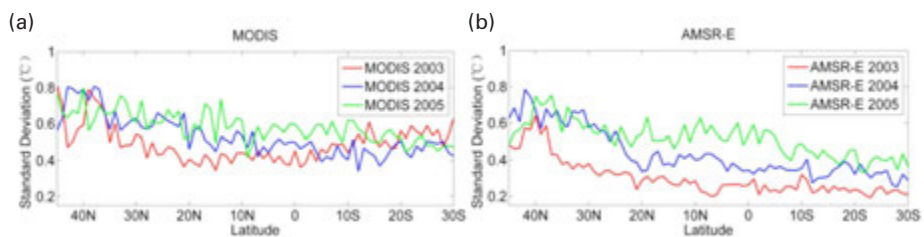


Fig. 18. Spatial tendency of RMSE in each year for MODIS SSTs and AMSR-E SSTs: (a) MODIS and (b) AMSR-E.



penetration, spatial resolution, the retrieval algorithm and the measured depth. The annual mean biases for both products are within 0.5 °C. Annual means of MODIS SSTs during 2003–2005 are cooler than those of drifting buoy SSTs, and those of AMSR-E SSTs are close to those of drifting buoy SSTs because MODIS SSTs represent the skin SST. Compared to the AMSR-E SSTs, the MODIS SSTs are much cooler than drifting buoy SSTs because MODIS represents skin SST whereas AMSR-E represents sub-skin SST. The intra-annual variation of the error of MODIS SSTs is much larger than that of AMSR-E SSTs, but the temporal tendencies of MODIS SSTs and AMSR-E SSTs do not change from year to year within this three-year period. This demonstrates the temporal stability of the errors in these two satellite SSTs products during the three-year study period. We also conclude that the error features of both MODIS SSTs and AMSR-E SSTs show obvious geographical variations. The accuracy and the precision become higher moving from north to south, and the amount of spatial variation of error features at all latitudes are larger than those of temporal variations.

Through our analysis we can see that the error features of satellite-derived SSTs show obvious spatio-temporal variations. Therefore, assuming that the errors of satellite SSTs are constant in ocean data assimilation and numerical weather forecasting may lead to inconsistent errors in the outputs of models. The results in this paper can be useful reference information for data assimilation or atmospheric and oceanic research. In our further work we will implement our method in this study into the global validation of satellite SSTs for longer time periods.

## Acknowledgments

This work was supported by the Natural Science Foundation of China (No. 41271347) and the National Basic Research Program (973 Program) Project of China (No. 2013CB733403). We would like to express our sincere gratitude to the people who provided excellent comments and valuable suggestions in the preparation of this manuscript. Special thanks to Emily Kang for her constructive comments and her help in polishing English to this manuscript.

## References

Abe, K. 1984. Evaluation of GMS-derived sea surface temperature in the southern hemisphere. *Aust. Meteorol. Mag.*, 32, 55–74.

Aihua Li, Y.B., Yuxin Zhu, Peng Guoa, Jian Bia, Yaqian He. 2013. Blending Multi-resolution Satellite Sea Surface Temperature (SST) Products Using Bayesian Maximum Entropy Method. *Remote Sensing of Environment*, 135, 52–63.

Dong, S., S.T. Gille, et al. 2006. Validation of the Advanced Microwave Scanning Radiometer for the Earth Observing System (AMSR-E) sea surface temperature in the Southern Ocean. *J. Geophys. Res.*, 111, C04002.

Dong, S., J. Sprintall, et al. 2006. Location of the Antarctic Polar Front from AMSR-E Satellite sea surface temperature measurements. *Journal of Physical Oceanography*, 36, 2075–89.

Donlon, C., P. Minnett, et al. 2002. Toward improved validation of satellite sea surface skin temperature measurements for climate research. *J. Clim.*, 15, 353–69.

Donlon, C. J. and GHRSSST-PP Science Team. 2005. The GHRSSST-PP product user manual. Exeter, UK, Int. GHRSSST-PP Project Off. GDS-v 1.5.

Gentemann, C. L., C. J. Donlon, et al. 2003. Diurnal signals in satellite sea surface temperature measurements. *Geophys. Res. Lett.*, 30, 1140.

Gentemann, C. L., F. J. Wentz, et al. 2004. In situ validation of Tropical Rainfall Measuring Mission microwave sea surface temperatures. *J. Geophys. Res.*, 109, C04021.

Guan, L. and H. Kawamura. 2003. SST availabilities of satellite infrared and microwave measurements. *J. Oceanogr.*, 59, 201–9.

Guoxiong, W., L. Jianping, et al. 2006. The key region affecting the short-term climate variations in China: The joining area of Asia and Indian-Pacific ocean. *Advances in Earth Science*, 21, 1109–18.

Høyer, J. L., I. Karagali, et al. 2012. Multi sensor validation and error characteristics of Arctic satellite sea surface temperature observations. *Remote Sensing of Environment*, 121, 335–46.

Kim, E. J., S. K. Kang, et al. 2010. Satellite-derived SST validation based on in-situ data during summer in the East China Sea and western North Pacific. *Ocean Science Journal*, 45, 159–70.

Lee, M. A., Y. Chang, et al. 2005. Validation of satellite-derived sea surface temperatures for waters around Taiwan. *Terrestrial, Atmospheric and Oceanic Sciences*, 16, 1189–204.

Li, X., W. Pichel, et al. 2001. Validation of coastal sea and lake surface temperature measurements derived from NOAA/AVHRR data. *International Journal of Remote Sensing*, 22, 1285–303.

Minnett, P.J., M. Smith, et al. 2011. Measurements of the oceanic thermal skin effect. Deep Sea Research Part II: Topical Studies in *Oceanography*, 58, 861–8.

Qiu, C., D. Wang, et al. 2009. Validation of AVHRR and TMI-derived sea surface temperature in the northern South China Sea. *Continental Shelf Research*, 29, 2358–66.

Reynolds, R.W. 1993. Impact of Mount Pinatubo aerosols on satellite-derived sea surface temperatures. *J. Clim.*, 6, 768–74.

Reynolds, R.W., C. L. Gentemann, et al. 2010. Evaluation of AATSR and TMI satellite SST data. *J. Clim.*, 23, 152–65.

Senan, R., D. Anitha, et al. 2001. Validation of SST and windspeed from TRMM using North Indian Ocean moored buoy observations. CAOS Report 2001AS1: 30 pp.

Stammer, D., F. Wentz, et al. 2003. Validation of microwave sea surface temperature measurements for climate purposes. *J. Clim.*, 16, 73–87.

Sun, F., C. Zhang, et al. 2007. Primary Validation of AVHRR/MODIS/TMI SST for Part of the Northwest Pacific. *Journal of Xiamen University (Natural Science)*, S1, 1–5.

Wentz, F.J., C. Gentemann, et al. 2000. Satellite measurements of sea surface temperature through clouds. *Science*, 288, 847–50.

Zhang, H., R. Reynolds, et al. 2009. An integrated global observing system for sea surface temperature using satellites and in situ data. *Bull. Am. Meteorol. Soc.*, 90, 31–8.